Topological dominance in peripheral vision

Ruijie Wu
State Key Laboratory of Brain and Cognitive Science, Institute of Biophysics, Chinese Academy of Sciences, Beijing, China

Bo Wang
State Key Laboratory of Brain and Cognitive Science, Institute of Biophysics, Chinese Academy of Sciences, Beijing, China
Hefei Comprehensive National Science Center, Institute of Artificial Intelligence, Hefei, China
University of Chinese Academy of Sciences, Beijing, China

Yan Zhuo
State Key Laboratory of Brain and Cognitive Science, Institute of Biophysics, Chinese Academy of Sciences, Beijing, China
University of Chinese Academy of Sciences, Beijing, China

Lin Chen
State Key Laboratory of Brain and Cognitive Science, Institute of Biophysics, Chinese Academy of Sciences, Beijing, China
Hefei Comprehensive National Science Center, Institute of Artificial Intelligence, Hefei, China
University of Chinese Academy of Sciences, Beijing, China
CAS Center for Excellence in Brain Science and Intelligence Technology, Shanghai, China

The question of what peripheral vision is good for, especially in pattern recognition, is one of the most important and controversial issues in cognitive science. In a series of experiments, we provide substantial evidence that observers' behavioral performance in the periphery is consistently superior to central vision for topological change detection, while nontopological change detection deteriorates with increasing eccentricity. These experiments generalize the topological account of object perception in the periphery to different kinds of topological changes (i.e., including introduction, disappearance, and change in number of holes) in comparison with a broad spectrum of geometric properties (e.g., luminance, similarity, spatial frequency, perimeter, and shape of the contour). Moreover, when the stimuli were scaled according to cortical magnification factor and the task difficulty was well controlled by adjusting luminance of the background, the advantage of topological change detection in the periphery remained. The observed advantage of topological change detection in the periphery supports the view that the topological definition of objects provides a coherent account for object perception in peripheral vision, allowing pattern recognition with limited acuity.

Introduction

One of the most basic characteristics of the human visual system is the distinction between foveal and peripheral vision (Rosenholtz, 2016; Strasburger, Rentschler, & Jüttner, 2011; Wertheim, 1894). Many previous studies suggest that foveal and peripheral vision might be fundamentally different and possibly designed for different visual functions. The fovea is good at processing fine spatial information due to high

Citation: Wu, R., Wang, B., Zhuo, Y., & Chen, L. (2021). Topological dominance in peripheral vision. *Journal of Vision*, *21*(10):19, 1–14, https://doi.org/10.1167/jov.21.10.19.

https://doi.org/10.1167/jov.21.10.19 Received December 30, 2020; published September 27, 2021 ISSN 1534-7362

spatial resolution, while the peripheral visual field is more sensitive to temporal properties (Carrasco et al., 2003). Although the peripheral visual field subtends more area in the whole visual field than the central visual field and participates in many visual tasks, it has a significant loss of information (Rosenholtz, 2016). When flanked by other items, the discrimination of a target deteriorates severely in peripheral vision, which is known as the crowding effect (Levi, 2008). The crowding effect cannot be accounted for by the loss of spatial resolution in the peripheral vision (Lettvin, 1976). Peripheral vision is involved in many visual tasks. For a range of visual tasks, the behavioral performance declines with retinal eccentricity, such as visual acuity and contrast sensitivity (Pointer & Hess, 1989; Rovamo & Virsu, 1979), line orientation discrimination (Makela, Whitaker, & Rovamo, 1993), contour integration (Hess & Dakin, 1997, 1999), shape detection (Achtman, Hess, & Wang, 2000; Nugent, Keswani, Woods, & Peli, 2003), mirror symmetry detection (Saarinen, 1988), and face identification (Melmoth, Kukkonen, Makela, & Rovamo, 2000). The different performance between the central and peripheral vision shown in these studies can be considered quantitative changes. These changes could result from the differences in factors such as reduced neural sampling rates or larger receptive fields. According to these factors, "cortical magnification factor" can scale the size of the peripheral stimuli, and then, the number of the neurons in response to peripheral stimuli was equivalent to the number of neurons in response to central stimuli. Performance on some visual tasks was successfully made up or improved by the scaling factor (e.g., Rovamo & Virsu, 1979, Sarrainen, 1988). However, some other studies showed clear failures of the scaling factor (e.g., Levi & Klein, 1986; Strasburger et al., 1991, 1994).

On the other side, with regard to stimulus appearance, in some visual aftereffects, the magnitude increases with eccentricity. These aftereffects include motion aftereffects (Castet, Keeble, & Verstraten, 2002), tilt aftereffects (Harris & Calvert, 1985), shape aftereffect (Gheorghiu, Kingdom, Bell, & Gurnsey, 2011), and face aftereffect (Tangen, Murphy, & Thompson, 2011). As a contextual effect, surround suppression is greatly amplified in the periphery (Xing & Heeger, 2000).

To understand our visual processing, we must understand peripheral vision. From Lettvin (1976) to Rosenholtz (2014), they described the peripheral processing of visual information as texture perception. Rosenholtz (2014) proposed that texture is statistical essentially, and it can more compactly be represented by its summary statistics than by the configuration of its parts.

The statistical inference approaches explain ambiguous perception from uncertain retinal images in periphery, whereas the topological perception theory attempts to highlight stability amid large variability in visual input. Chen's global topological perception theory states that the primitives of visual form perception are geometric invariants at different levels of structural stability under transformations (Chen, 1982, 2005). This theory argued that the core intuitive notion of an object is its holistic identity preserved over shape-changing transformations. This identity can be characterized precisely as topological invariance. Topological transformations can be imagined as an arbitrary "rubber-sheet" distortion, in which neither breaks nor fusions can happen, but changes in shape of the "rubber-sheet" may be. Under this kind of "rubber-sheet" distortion, connectivity, the number of holes, and the inside/outside relationship remain invariant. Hence, they are topological invariants, while local features altered over such shape distortion, such as orientation, size, and shape, are not. To explore what information can be remained and then processed in peripheral vision, the global-first topological approach (Chen, 2005) was tested in this article. The topological approach to perceptual organization provides a new definition of global versus local and a new perspective in viewing the formation of an object. Chen and his colleagues' research indicates the general and abstract nature of holes in the formation of new objects, independent of detailed geometric or physical properties (Wang et al., 2007; Zhou et al., 2010; Zhuo et al., 2003). A basic issue in applying topology to the study of perceptual organization is how to describe global properties in a discrete set. With the aid of the mathematics of tolerance spaces (algebraic topology–homology theory) developed by Zeeman (1962), this topological approach is developed to apply global tolerance properties (rather than general topology) to define the global properties in a discrete set (Chen, 2005). Thus, perceptual organization, including Gestalt laws of proximity and similarity, may be described in a unified manner by global tolerance (topological) properties (Chen, 2005). Our previous finding revealed that the topological difference between target and flankers could alleviate crowding effect (Xi, Wu, Wang, & Chen, 2020). The topological property plays a role in perceptual grouping, which modulates the crowding effect.

Since the detection of topological properties does not require fine spatial details, and the topological approach emphasizes a "global-first" approach to perceptual organization, the peripheral visual system could easily detect topological change in holes as the emergence of a new object, which will guide spatial attention and fixation to a new object. A key, but counterintuitive, prediction of form vision in the periphery is that the topological change of a figure (e.g., the appearance of a hole in a solid figure) plays an overarching role in object perception in peripheral vision. We wondered what is lost from the form and what remains to be detected and then processed. Our principal goal was to

better understand pattern recognition in the peripheral visual field, which determines the key factor of object formation in the periphery.

Experiments: Methodological overview

In total, there were 142 students who participated in the study. Each student participated in one of the six experiments. They reported normal or corrected-to-normal vision and were paid for their participation. Before participating in an experiment, they were unaware of the purpose of the experiment.

Participants were seated in a dimly lit room in front of a CRT monitor. A chinrest held the participant's head steadily. The stimuli were shown on a Dell computer with a 22-in. CRT monitor with 1,024 × 768 resolution. The vertical refresh rate of the monitor was 60 Hz for all experiments. The display was placed at a distance of 56 cm in front of the subjects. MATLAB software (MathWorks, Inc.) with the Psychophysics Toolbox PTB-3 (Brainard & Vision, 1997) was used to display stimuli and record responses.

Experiment 1: Sensitivity assessment

Experiment 1 assessed the sensitivity to perceive changes in the number of holes in the patterns displayed in parafovea and peripheral vision using a change detection task during continuous motion of stimulus. The term *change detection* pertains primarily to visual processes involved in first noticing a change. It denotes only detection proper (i.e., the observers reporting the existence of the change). The perception of dynamic patterns per se (e.g., the perception of movement) is not discussed here. A bias-free index, d', was applied to quantify the sensitivity of change detection.

Method

Participants

There were eight undergraduate participants who participated as subjects in each of the seven experiments (1a: four females, one left-handed, age 18–22 years; 1b: five females, age 19–22 years; 1c: four females, age 19–21 years; 1d: three females, one left-handed, age 20–23 years; 1e: four females, age 19–23 years; 1f: five females, age 20–23 years; 1g: four females, age 18–23 years).

Stimuli

The stimuli were black shapes, displayed on a gray background. The displays appeared on a gray background and consisted of a green cross in the center of the screen as the fixation point throughout the experiment. The black stimuli subtended a size of 3.5° high × 3.5° wide. The shape of the stimuli varied between all of the seven experiments to control for the shape factor. On each trial, four stimuli in continuous vertical motion were simultaneously and bilaterally presented at an eccentricity of 5° and 20°. The background luminance was manipulated block by block to avoid ceiling effects and obtain a stable level of performance.

Design

The experiment was a 2 × 2 within-subjects design. The principal manipulations were stimulus locations (5° [i.e., central visual field] vs. 20° [i.e., peripheral visual field]), and the type of shape changes (changes with holes or changes in number of holes as topological change vs. changes without hole as nontopological change). Because our main concern was the influence of eccentricity, for each subject, we had "nontopological change" blocks and "topological change" blocks, and in each block, four stimuli appeared bilaterally at both of the two eccentricities (5° and 20°) simultaneously. In each block, each participant completed 392 trials, among which 196 trials were motion with change and 196 trials were motion without change. Among the trials with a change, 98 trials were those where change occurred at the eccentricity of 5°, and 98 trials were those where change occurred at the eccentricity of 20°. If the subject correctly identified both the change and the item on which the change occurred, this trial was labeled a "hit" trial of the corresponding condition. If the subject falsely reported a no-change trial as a change one, according to the location of the item the subject reported, this trial was labeled a "false alarm" trial of the corresponding condition.

Each participant underwent two to four blocks on average, including one block with a topological change task and at least one practice block with nontopological change.

Procedure

The observers were read instructions specifying the task, advising them to fixate on the fixation point throughout the experiment, and requiring them to respond whether there was a change and accurately identify which of the four stimuli underwent the change. Before the experiment, the observers completed calibration of the eye-tracking system and were trained to keep fixation for at least 4 s.

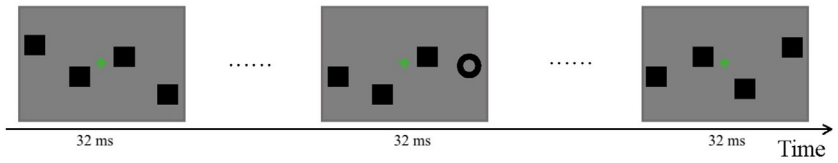

Figure 1. Illustration of the change detection paradigm used in Experiments 1, 2, and 3. The initial screen display with four identical figures at four random locations of 5° and 20°. As the motion continued, at a random moment, one of the items underwent a transient shape change (e.g., a square to ring). This new display presented for 32 ms and the ring changing into a square with continuous motion until the end of the trial.

For practice, several nontopological change blocks preceded the experiment. In the first block, if the performance of the "nontopological change" at 20° exceeded a d' of 2.5, the background luminance was set lower for the next block. If the performance of the "nontopological change" was below a d' of 1, the task was made easier by raising the background luminance.

The observer pressed a key to initiate each trial. Along an invisible vertical trajectory, the stimuli moved 13 arcmin in a row and stayed at each spot for 32 ms, which appeared as a smooth motion at a speed of 10.8 degree/s for 2 s per trial. The stimuli started to move from different positions and in different directions (either upward or downward) randomly. During the animation, in half of the trials, there was a transient shape change on one of the four stimuli. The new figure was presented for only 32 ms and replaced by a previous figure as the motion continued and then stopped (Figure 1).

In this experiment, subjects' eye movements were monitored using an SMI eye tracker. Eye gaze was monocularly recorded at 120 Hz. The eye tracker was calibrated by requiring the participants to fixate on a number of points evenly distributed on the screen. During each trial, if the pupil position shifted away from the fixation point by about 2.5°, this trial was marked as invalid, and the exact same trial would be added to the end of this block. If for a certain block, there were more than 10 (5%) invalid trials, that observer's data were marked as invalid.

Results

To evaluate the performance of change detection in the central and peripheral visual field, a two-way within-subjects analysis of variance (ANOVA; eccentricity [5° vs. 20°] × type of change [topological change vs. nontopological change]) was performed on the psychophysical index of d'.

Experiment 1a measured the general performance of topological change detection, using the stimuli of a square changing to a ring as the topological change and a square to a disk as the nontopological change. As shown in Figure 2a, the d' of the topological change was larger in the peripheral condition while the d' of the nontopological change was smaller in the periphery (the interaction between eccentricity and type of change: $F_{(1,\ 7)} = 35.89$, $p < 0.001$, $\eta_p{}^2 = 0.84$). The topological change detection at 20° was found to be significantly more sensitive than it was at 5° ($t_{(7)} = -4.97$, $p = 0.002$, Cohen's $d = -1.79$) , while the nontopological change was impaired at 20° ($t_{(7)} = 5.28$, $p < 0.001$, Cohen's $d = 1.87$).

In Experiment 1b, we tested one of the conditions of the topological changes, a transformation of a disk to a ring. Because the ring has a hole and the disk does not, the transition between the disk and the ring represents a change in topology. Moreover, since the disk and ring share the same outer contour shape, they seem more similar than the square and ring, and thus we were able to eliminate the factor of similarity of shape. A transformation of a disk to a square represented a nontopological change. The interaction between the eccentricity and type of change was significant (ANOVA: $F_{(1,\ 7)} = 61.5$, $p < 0.001$, $\eta_p{}^2 = 0.89$). The topological change at 20° showed a better performance than it did at 5° ($t_{(7)} = -5.41$, $p = 0.002$, Cohen's $d = -1.93$), while the detection of the nontopological change was better at 5° ($t_{(7)} = 4.59$, $p = 0.003$, Cohen's $d = 1.63$) (Figure 2b).

A potential confounding factor in the disk-ring transition may be that the appearance and disappearance of a hole could affect other features. In Experiment 1c, the ring and S-shape figure were made to have equal area (and therefore luminous flux), very nearly the same spatial frequency components and perimeter length, and equal averaged edge crossings. The shape of the S-shape figure was also manipulated to be irregular to eliminate possible effects of subjective contours. A square to a disk transformation represented a nontopological change. The performance of the topological change detection in the periphery was superior to that of the central presentation (the interaction between eccentricity and change type:

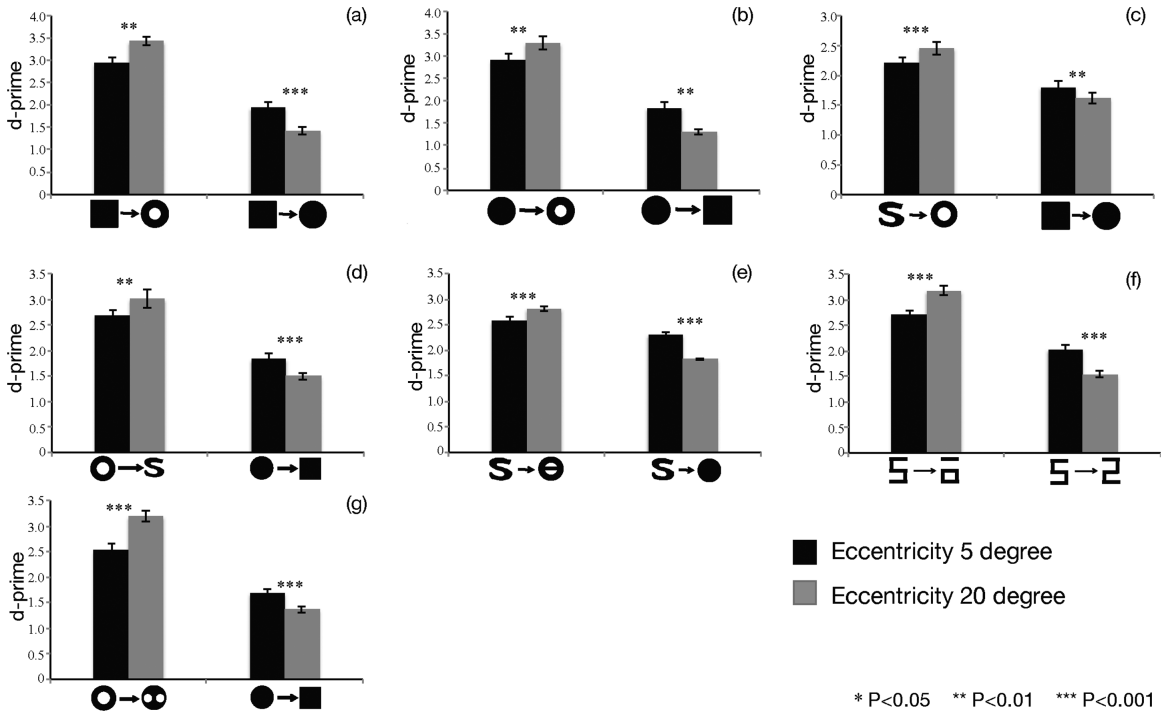

Figure 2. (a–g) Results of Experiments 1a to 1g. Each panel shows mean behavioral performance of the change detection tasks. The performance was measured by d' shown in the ordinate. On each panel, the results are shown for two eccentricity conditions of topological change (left two columns) and nontopological change (right two columns). The schematic depiction of the stimulus pairs for each condition is presented on the abscissa. Error bars indicate standard error of the mean.

$F_{(1,\ 7)} = 104.65$, $p < 0.001$, $\eta_p^2 = 0.94$). The detection of topological change was better at 20° than at 5° ($t_{(7)} = -6.18$, $p < 0.001$, Cohen's $d = -2.21$), while the detection of nontopological change was better at 5° than 20° ($t_{(7)} = 3.60$, $p = 0.009$, Cohen's $d = 1.22$) (Figure 2c).

In terms of topology, both the changes of a solid figure to a hollow one and its reverse, the change of a hollow figure to a solid one, represent a topological change in holes. Considering the symmetric nature of topological changes, Experiment 1d was performed with the initial ring–S-shape figure switch instead of the initial S-to-ring switch. A disk-to-square transformation represented a nontopological change. Topological change detection was found to be more sensitive in the periphery (interaction between eccentricity and change type: $F_{(1,\ 7)} = 24.07$, $p = 0.002$, $\eta_p^2 = 0.78$). Topological change detection was better at 20° than at 5° ($t_{(7)} = -4.08$, $p = 0.005$, Cohen's $d = -1.43$), while the d' of the nontopological change detection was worse at 20° ($t_{(7)} = 5.05$, $p < 0.001$, Cohen's $d = 1.80$) (Figure 2d).

One of the primary concerns in the study of change detection is the role played by local cues in distinguishing visual patterns. Thus, it could be argued that the discrimination capacity observed in at least some of the above experiments may have been distinguished from the S-shape figure on the basis of the fact that the ring has a white region in the middle that may stimulate an on-center cell, or the S-shape figure could have been distinguished from the ring on the basis that the S-shape figure has an oriented, straight-line segment in the middle. To address these possibilities, a θ-shape form (hereafter referred to as θ) was applied to replace the ring in Experiment 1e. The θ was designed by adding a central bar to a ring-shape shape such that it had no white part at its center. The θ and S also were made to have the same area and were oriented such that their central bars were parallel. Because the θ has two holes and the S has none, they still differ topologically with regard to the presence of holes, and the S-θ transition also controlled for on-center cell detector, edge energy, horizontally oriented spatial frequency components, and luminous flux. In previous experiments, even though the S-to-ring pair controlled well for various local feature properties, the topological account still may be challenged by one further counterexplanation: The sensitivity might not be caused by the topological change in holes per se but by the fact that the shape transformations of the S-to-ring, square-ring, and disk-ring are more extensive than the shape transformation of the disk-square. In this experiment, we also used the S-disk transition as a nontopological change, which differs extensively in shape but is topologically equivalent. Moreover, the

area of S and θ was designed to be the same, while the area difference between the S and disk was larger than S and θ, and this could provide us with a control for differences in area. Topological change detection had better performance in the periphery (interaction of eccentricity and type of change, ANOVA: $F_{(1,\ 7)} = 232.23$, $p < 0.001$, $\eta_p^2 = 0.97$). The d' value of topological change at 20° was larger than at 5° ($t_{(7)} = -6.63$, $p < 0.001$, Cohen's $d = -2.19$), while the nontopological change detection became worse at 20° ($t_{(7)} = 8.10$, $p < 0.001$, Cohen's $d = 2.93$) (Figure 2e).

Although the S-to-ring change was designed to control for spatial frequency components, a potential issue remains that because the S carries a horizontally oriented bar in the middle, there is more horizontal-edge energy and higher horizontal spatial frequencies in the S than in the ring. Moreover, a neuron merely preferring horizontal edges or horizontal higher spatial frequencies could distinguish the S from the ring without explicitly analyzing topology. Additionally, the eye is not equally sensitive to contrast variations at all spatial and temporal frequencies; rather, the contrast sensitivity function is a bandpass filter for stimuli of low temporal frequency but is a low pass filter with large high spatial frequency losses for briefly presented or rapidly flickering stimuli moving on the retina (e.g., Wichmann & Henning, 1998). To address these issues, Experiment 1f designed a ⊟-shape figure and a ⊐-shape figure instead of the ring and the S, respectively. The ⊟-shape figure changed into a ⊐-shape figure representing nontopological change. The ⊟-shape, ⊐-shape, and ⊐-shape have the same horizontal line segments, the same number of terminators, and nearly the same spatial frequency content. Nonetheless, the results demonstrated that topological change detection was more sensitive in the peripheral visual field (interaction of eccentricity and type of change, ANOVA: $F_{(1,\ 7)} = 274.93$, $p < 0.001$, $\eta_p^2 = 0.98$; d' of topological change at 5° vs. at 20°: $t_{(7)} = -7.77$, $p < 0.001$, Cohen's $d = -2.79$; the d' of the nontopological change at 5° vs. at 20°: $t_{(7)} = 6.83$, $p < 0.001$, Cohen's $d = 2.44$) (Figure 2f).

The topological definition of perceptual objects has been tested against transitions between solid and hollow forms, including no hole to one hole and no hole to two holes. In Experiment 1g, we further generalized the topological change of one hole to two holes reflected in the change in the number of holes. To control for changes in local features, such as luminous flux, spatial frequency components, and perimeters, the sums of the areas of the two small holes contained in the two-hole disk were made to be equal to the area of the big hole contained in the ring. Nontopological change was represented by the disk-square transition. Consistent with Experiments 1a to 1f, the detection of the topological change showed a better performance in the periphery (interaction of eccentricity and type of change, ANOVA: $F_{(1,\ 7)} = 118.35$, $p < 0.001$, $\eta_p^2 = 0.94$). The d' value of topological change at 20° was larger than at 5° ($t_{(7)} = -7.16$, $p < 0.001$, Cohen's $d = -2.52$), while nontopological change detection was impaired in the periphery ($t_{(7)} = 13.90$, $p < 0.001$, Cohen's $d = 4.81$) (Figure 2g).

Experiment 2: Controlling for task difficulty

The previous experiments that controlled for shape factors consistently suggested that the detection of topological change was more sensitive at 20° than that at 5°, while the detection of the nontopological change was impaired at 20°. Despite this, it may be argued that the topological change task was easier than the nontopological change task, which could account for the difference we found in the periphery.

In the previous experiments, for topological change blocks, the d' of the central visual field was smaller than that of the periphery, whereas for the nontopological change blocks, the d' of the peripheral visual field was smaller than that of the central visual field. We manipulated the luminance contrast to match the task difficulty of the conditions with the lower performance in both of the two blocks that were tested before. The data pattern showed topological dominance in the peripheral condition, consistent with previous results.

Method

Participants

In all five experiments (Experiments 2a–2e), 60 undergraduates participated as paid observers (2a: 12 participants, 5 females, age 18–23 years; 2b: 12 participants, 7 females, 1 left-handed, age 18–23 years; 2c: 12 participants, 6 females, age 19–22 years; 2d: 12 participants, 6 females, age 18–22 years; 2e: 12 participants, 5 females, 1 left-handed, age 18–22 years).

Stimuli and design

The apparatus and stimuli were identical to those in Experiment 1. A lower luminance contrast was adopted to obtain a low light level, under which the observers underwent the "topological change block." The luminance contrast varied block by block to obtain a d' for topological change detection at 5° approximately around 3. On the other hand, we raised the luminance contrast block by block until the d' at

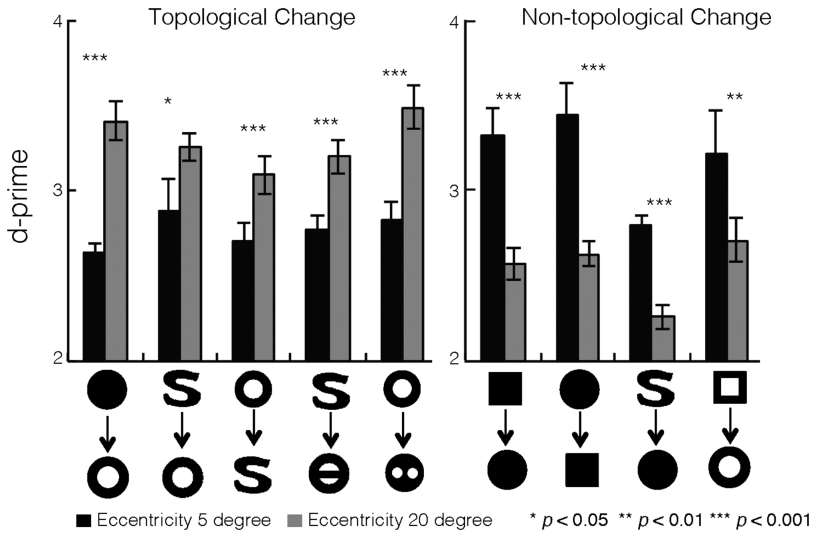

Figure 3. Mean change detection performances of the five experiments (Experiments 2a to 2e). The results are shown in two grouped categories of topological changes and nontopological changes. In this experiment, the background luminance for the topological change condition was set lower than that of the nontopological change condition. The schematic depiction of the stimulus pairs for each condition was presented on the abscissa. Error bars indicate standard error of the mean.

20° for nontopological change detection was between 2 and 3. The general design was the same as Experiment 1 except that each participant underwent two to six blocks on average, including several blocks with the topological change task and at least one block with the nontopological change task.

Procedure

The general procedure was the same as Experiment 1. In this experiment, we decreased the luminance contrast for the topological change detection in the central visual field to reduce the d' value to between 2 and 3 and raised the luminance contrast to improve the d' of the nontopological change detection in the periphery to between 2 and 3. Although the luminance contrast was different for the topological and nontopological change task, we obtained matched task difficulty for these two tasks as quantified using the d'. Under different physical conditions, we tried to observe how the pattern of performance varied across the visual field in the topological change task and nontopological change task.

Results

The results of Experiment 2 are shown in Figure 3. In Experiment 2a, we employed the disk-to-ring transition to represent topological change and the disk-to-square transition for nontopological change. We observed a significant interaction between the factors of eccentricity and type of change (ANOVA: $F_{(1,\ 11)} = 130.69$, $p < 0.001$, $\eta_p^2 = 0.92$). The detection of topological change was better at 20° than 5° ($t_{(11)} = -7.96$, $p < 0.001$, Cohen's $d = -2.30$). In contrast, the detection of nontopological change was impaired at the periphery ($t_{(11)} = 5.36$, $p < 0.001$, Cohen's $d = 1.55$).

In Experiment 2b, we used the hollow square to hollow ring transition to represent nontopological change and the S-to-ring transition as topological change to exclude the possibility that the impaired performance might be caused simply by the difficulty in detecting hollow figures (i.e., rings) rather than by the topological change in holes per se. A significant interaction still existed (ANOVA: $F_{(1,\ 11)} = 27.05$, $p < 0.001$, $\eta_p^2 = 0.71$). Topological change detection was better at 20° than at 5° ($t_{(11)} = -2.71$, $p = 0.02$, Cohen's $d = -0.74$), while nontopological change detection at 20° was worse than that at 5° ($t_{(11)} = 2.15$, $p = 0.05$, Cohen's $d = 0.62$).

Both the change of a solid figure to a hollow one and its reverse, the change of a hollow figure to a solid one, can define a topological change. In order to control for the symmetric nature of topological changes, Experiment 2c was designed with an initial ring-to-S switch instead of an initial S-to-ring switch. The disk-to-square transition was used as a nontopological change. Consistent with previous experiments, the detection of topological change was more sensitive at 20° than that at 5° ($t_{(11)} = -6.69$, $p < 0.001$, Cohen's $d = -1.93$); however, the detection of nontopological change was worse in the periphery than in the central visual field ($t_{(11)} = 5.13$, $p < 0.001$, Cohen's $d = 1.48$). This result supported the previously found advantage for topological change detection in peripheral vision (ANOVA: $F_{(1,\ 11)} = 47.10$, $p < 0.001$, $\eta_p^2 = 0.81$).

In Experiment 2d, a θ-shape form (hereafter referred to as θ) was applied to replace the ring. In this experiment, we also tested the S-disk transition, which differs extensively in shape but is topologically equivalent. The interaction between eccentricity and type of change was significant (ANOVA: $F_{(1,\ 11)} = 154.09$, $p < 0.001$, $\eta_p^2 = 0.93$). In the periphery, the detection of topological change was better than that of nontopological change ($t_{(11)} = -5.86$, $p < 0.001$, Cohen's $d = -1.69$), but the nontopological change showed the opposite trend in that it was better detected in the central visual field ($t_{(11)} = 9.82$, $p < 0.001$, Cohen's $d = 2.83$).

In Experiment 2e, we used a two-hole disk turning into a ring as the topological change condition. To control for changes in local features, the sums of the areas of the two small holes contained in the two-hole disk were equal to the area of the big hole contained in the ring. Nontopological change was represented by the square-disk transition. The detection of the topological change was more sensitive at the peripheral location than at the central location ($t_{(11)} = -6.49$, $p < 0.001$, Cohen's $d = -1.87$). However, nontopological change detection was better at 5° than at 20° ($t_{(11)} = 5.86$, $p < 0.001$, Cohen's $d = 1.69$). A significant interaction between eccentricity and type of change was revealed (ANOVA: $F_{(1,\ 11)} = 56.39$, $p < 0.001$, $\eta_p^2 = 0.84$).

In Experiments 2a to 2e, we manipulated the luminance of the background to match the task difficulty for topological and nontopological changes tasks. We used five pairs of figures to control for shape factors. The results showed that even when the detection of nontopological change was made easier, the previously found patterns of the performance both in the periphery and in the central visual field were not changed. The advantage of detecting topological change nonetheless existed in the periphery, and the detection of nontopological change was still better in the central visual field rather than in the periphery. These findings were consistent with those in Experiment 1, where the detection of topological change was better in peripheral vision than in the central visual field.

Experiment 3: Applying cortical magnification in the periphery

More areas and neurons are devoted to the central visual field than to the peripheral regions, from retinal ganglion cells to visual cortex (Azzopardi, Jones, & Cowey, 1999; Lennie, 1998). Many studies confirmed that the M-scaling could make up for the poor resolution peripherally. The performance of grating acuity (Rovamo & Virsu, 1979), Snellen acuity (Virsu, Näsänen, & Osmoviita, 1987), and orientation discrimination (Thomas, 1987) could be compensated by cortical magnification. However, in a study by Carrasco et al. (2003), peripheral performance was better, the speed of information processing being higher when the same-size stimuli appeared at 9° than at 4°; opposite to what is normally found, that difference was attenuated when the 9° stimuli were magnified to equate cortical representation size. In this experiment, we explored whether the topological sensitivity was changed when the stimuli were magnified.

Method

Participants

The observers were eight (four females, age 19–23 years) college students who were paid for their effort and time.

Stimuli

The stimuli were the same as those in Experiment 1c, a square to disk transition representing nontopological change and a S-shape to ring transition as topological change. At the eccentricity of 5°, the size of the stimuli remained at 3.5°, and at the eccentricity of 20°, the size of the stimuli was scaled to 10.7° (Rovamo & Virsu, 1979). On each trial, four figure stimuli in continuous vertical motion were simultaneously and bilaterally presented at eccentricities of 5° and 20°.

Design and procedure

The design was the same as that in Experiment 1. In this experiment, we first ran two luminance contrast threshold tests with nontopological change at an eccentricity of both 5° and 20°. There were two stimuli symmetrically displayed on the left and right of the fixation point for each trial. Their animation was similar to that seen in Experiment 1. With these threshold tests, we could set the two luminance contrast values for both central and peripheral location. Subsequently, four blocks of change detection tests were run, adopting the contrast luminance value measured before, to estimate the d' values for the four conditions (eccentricity [5° and 20°] × type of change [topological change and nontopological change]).

Results

Topological sensitivity is not diminished by magnification of the stimuli in the periphery. A significant interaction between eccentricity and type of change was also found (ANOVA: $F_{(1,\ 7)} = 25.54$, $p = 0.001$, $\eta_p^2 = 0.79$). Topological change detection at 20° was significantly better than that at 5° ($t_{(7)} = -2.37$, $p < 0.05$, Cohen's $d = -0.75$), while nontopological change detection was better at 5° than 20° ($t_{(7)} = 6.30$, $p < 0.001$, Cohen's $d = 2.73$). An overall main effect of topological

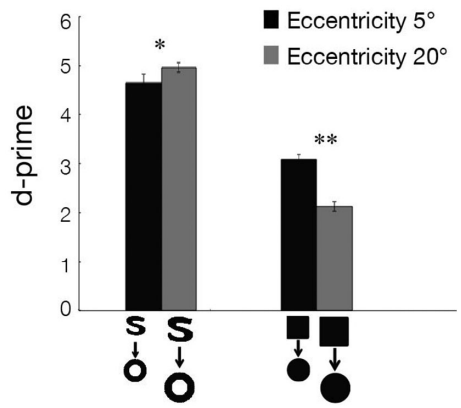

Figure 4. Results of Experiment 3. Schematic depiction of the stimulus pairs at the eccentricity of 5° and the scaled ones at the eccentricity of 20° is shown on the abscissa. Error bars denote the standard error of mean.

dominance both centrally and peripherally ($F_{(1,\ 7)} = 22.69, p = 0.002, \eta_p^2 = 0.76$) was also revealed (Figure 4).

Experiment 4: Expanding the eccentricity to 30°

In this experiment, we generalized a more natural and general scene to investigate change detection with moving items across eccentricities. Four stimuli were presented with random motion in different directions across the whole screen and kept away from each other during the animation. In a random motion paradigm, observers should distribute their attention across the whole screen. This made it difficult to predict the position where the change would occur. It is also more similar to natural environments where changes occur on an unpredicted position. We used an eccentricity of 30° as the peripheral measurement and 5° as the central measurement. The position at which an abrupt change happened was either at 5° or 30° within the radius of the fixation point.

Method

Participants

The observers were eight (five females, one left-handed, age 19–23 years) college students, who were paid for their effort and time.

Stimuli

The stimuli were identical to those in Experiment 1c. Four items at different positions started to move toward different directions, which was any direction in 360°. The minimum distance between two encountering items was 4° from center to center. The random motion lasted for 6 s. Between 0.5 and 5.5 s of the random motion, at a random time point, a topological change (in this experiment, we used the S-to-ring transition) or nontopological change (a square to disk transition) occurred transiently at an eccentricity of either 5° or 30° along the radial direction of the fixation point.

Design and procedure

The general design and procedure were the same as that in Experiment 1. At the beginning of each trial, subjects were required to maintain fixation on a green cross at the center of the screen during the whole trial time. The stimuli started moving from random positions on the screen and toward different directions without bumping into each other. In half of the total trials, an abrupt change happened at an eccentricity of either 5° or 30° in the radial direction. The performance was quantified by d'. If the change was noticed, the space key was pressed and the motion was paused. The subject was asked to point the mouse at the exact item to which the change occurred. If for one trial without any change, the response was "yes" to a change, the falsely detected position was calculated. Next, we estimated which potential change position (5° and 30°) was nearer to the falsely detected position. This trial would be labeled as a false alarm for the position of the same change type as this trial.

Results

Consistent with previous findings, a significant interaction between eccentricity and type of change was observed (ANOVA: $F_{(1,\ 7)} = 74.63, p < 0.001, \eta_p^2 = 0.91$). Topological change detection was better at 30° than at 5° ($t_{(7)} = -4.18, p = 0.004$, Cohen's $d = -1.46$). In contrast, nontopological change detection was worse at 30° than at 5° ($t_{(7)} = 7.37, p < 0.001$, Cohen's $d = 1.58$). This finding suggests that the superiority in detecting topological change at 20° is not a special case and that the topological advantage can be found in more eccentric areas in the peripheral visual field (Figure 5).

Experiment 5: Measuring at more eccentricities

Previous experiments consistently suggested topological dominance in the peripheral visual field. In this experiment, in order to investigate whether this phenomenon is a general principle, we performed measurements at more eccentricities using a random

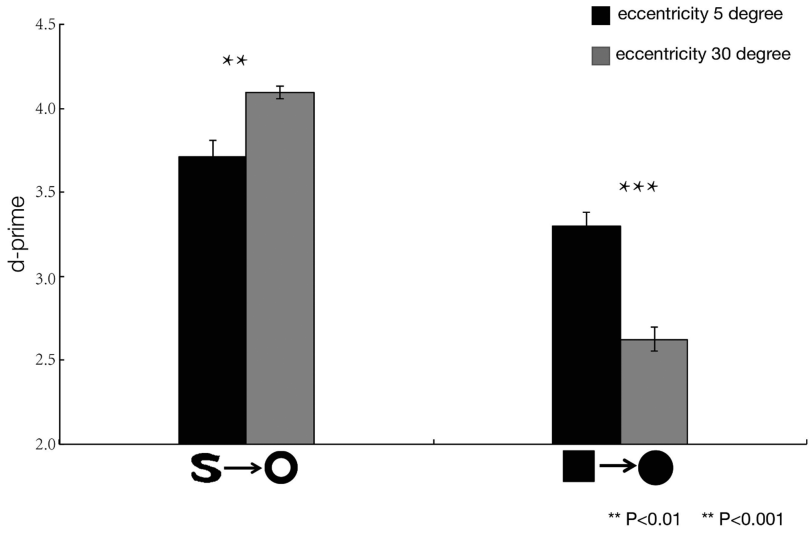

Figure 5. Results of Experiment 4. In this experiment, the eccentricities were 5° and 30° representing central vision and peripheral vision. Error bars denote the standard error of mean.

motion paradigm: 2°, 12°, and 26°. The S-to-ring transition was applied as a topological change and a square-to-disk transition as the nontopological change.

Method

Participants

The observers were 10 (6 females, age 18–22 years) college students, who were paid for their effort and time.

Stimuli

The stimuli and random motion were identical to those in Experiment 4. However, in this experiment, the potential change positions were at eccentricities of 2°, 12°, or 26°.

Design

Each participant completed one topological change block and one nontopological change block. In each block, there were 300 trials with a change during random motion and 300 trials without any change during a random motion. Of all 300 trials with a change, one third of which was that the change occurred at an eccentricity of 2°, one third at 12°, and one third at 26°.

Procedure

The d' value was used to measure the performance. The subjects were required to respond to whether there was an abrupt shape change during motion by pressing the space key and indicate for which item the change had occurred. If for one trial without any change, the response was "yes" to a change, the falsely detected position was calculated. We then estimated which potential change position (2°, 12°, or 26°) was closer to the falsely detected position. This trial would be labeled as a false alarm for this potential change position with the same change type as this trial.

Results

A significant interaction was also found (ANOVA: $F_{(2,\ 18)} = 142.87$, $p < 0.001$, $\eta_p^2 = 0.94$). The main effect of both the change of property and eccentricity was significant (change of property, topological change, and nontopological change, $F_{(1,\ 9)} = 211.68$, $p < 0.001$, $\eta_p^2 = 0.96$; eccentricity, 2°, 12°, and 26°, $F_{(2,\ 18)} = 104.85$, $p < 0.001$, $\eta_p^2 = 0.92$). The detection of topological change in the periphery was as good as in the central visual field (Bonferroni-corrected post hoc tests: $p > 0.1$). However, the d' of nontopological change detection was worse in the periphery (Bonferroni-corrected post hoc tests: 2° vs. 12°, $p = 0.31$; 2° vs 26°, $p < 0.001$; 12° vs 26°, $p < 0.001$) (Figure 6). This result is consistent with Experiments 1 to 4 that the detection of nontopological change was impaired at the periphery. The detection of topological change was always good regardless of where the stimuli were presented, and the detection remained better for all motion patterns tested. The data pattern still showed double dissociated of the topological change and nontopological change across eccentricities. Perhaps the range of eccentricities included resulted in the increase of task difficulty and attention load. Moreover, the d' value reached a ceiling

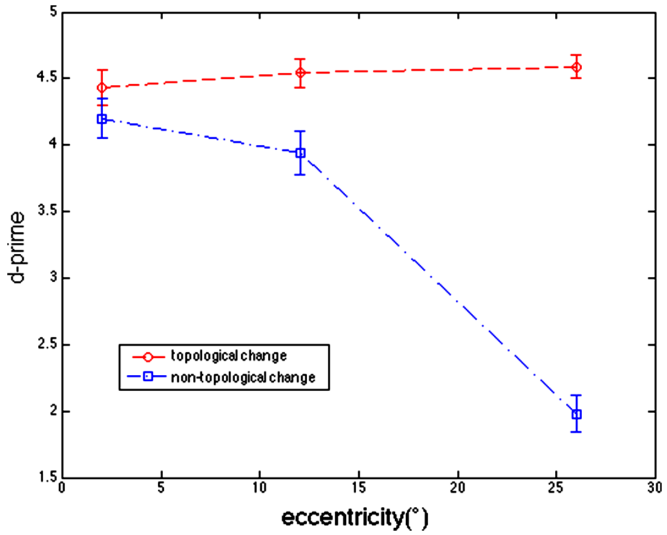

Figure 6. Average performance of change detection task measuring at 2°, 12°, and 26° with a random motion paradigm. Error bars represent standard error of the mean.

level for the topological change condition at all of the three eccentricities.

Discussion

All behavioral results consistently supported the topological dominance in peripheral vision. The topological account of perceptual objects was generalized to different kinds of topological transitions, including the transition from no hole to one hole, one hole to no hole, one hole to two holes, and no hole to two holes, all of which consistently showed a better performance in the periphery than in central vision. The form of motion varies, either along a fixed invisible vertical trajectory or in a random motion, but the behavioral performance for topological change detection remains better in the periphery. However, the behavioral performance for nontopological change detection deteriorates in the periphery.

A major challenge to topological perception is that there can be no two figures that differ only in topological properties without any differences in local features. Moreover, the fovea is superior in the perception of color and fine details (Boynton, 1979; Roedieck, 1973). Relative to the periphery, it has higher visual acuity, spatial resolution, and contrast sensitivity (Berardi & Fiorentini, 1991; Connolly & Van Essen, 1984). Thus, one cannot test for the role of peripheral vision in detecting topological change in complete isolation. We managed to minimize confounding factors of pattern recognition through elaborate design of the stimuli to prevent subjects from depending on nontopological properties during a topological change task.

The observed sensitivity advantage at more eccentric locations cannot be explained by peripheral sensitivity for temporal properties in the visual world (Hartmann, Lachenmayr, & Brettel, 1979). Both topological change and nontopological change were detected in motion, while they showed the opposite pattern for changes in sensitivity as eccentricity increased.

More areas and neurons are devoted to the central visual field than to the peripheral areas, from retinal ganglion cells to visual cortex (Azzopardi, Jones, & Cowey, 1999; Lennie, 1998). In our study, the advantage of topological change detection was not diminished by cortical-magnification scaling of the stimulus and was about the same as with unscaled stimuli. When stimuli were scaled according to cortical magnification, the d' of topological change detection still remained better in the periphery. This shows that the advantage of peripheral vision to topological changes is not removed by scaling the image size according to spatial variation in the mapping of the retinae onto the cortex.

In macaque monkeys and cats, the speed of conduction and integration time are about 20 ms faster for magnocellular neurons than for parvocellular neurons (Lamme & Roelfsema, 2000; Schmolesky et al., 1998), and the ratio of parvocellular cells: magnocellular cells (P:M) decreases with eccentricity (Azzopardi, Jones, & Cowey, 1999). The magnocellular pathway is known to convey low-resolution, achromatic information rapidly (Chen et al., 2006; Maunsell, Nealey, & dePriest, 1990). However, the parvocellular and many of fewer koniocellular neurons conduct information more slowly and can resolve fine details and chromatic contrast but require substantially higher luminance contrast. Moreover, functional magnetic resonance imaging studies have suggested that magnocellular projections generate "initial guesses" based on magnocellular-biased information (Kveraga, Boshyan, & Bar, 2007). On the other hand, topological perception theory proposes that the extraction of topological properties serves as the starting point of object perception (Wang et al., 2007). The observed topological dominance in the periphery might be the result of the different spatiotemporal characteristics of the M and P pathways. Since the detection of topological change does not require fine spatial details, it is similar to the magnocellular-biased information to some extent. In the future, we need to investigate the relationship between topological properties and nontopological properties conveyed via the magnocellular pathway. Evidence of topological properties mainly conveyed via the magnocellular pathway could provide explanation to our results of topological dominance in the periphery.

Studies of symmetry detection in the periphery showed a faster drop of detectability with increasing eccentricity for constant-size patterns than that for M-scaled patterns (Sarrinen, 1988). However, the stimuli they used were distributed dots patterns that required a point-by-point comparison to detect mirror symmetry. For closed patterns, which have low spatial frequencies, the symmetric relations can be extracted globally (Carmody, Nodine, & Locher, 1977). This might be consistent with the topological properties that can be extracted globally and does not require high spatial resolution. In the future, mirror symmetry detection in the periphery with closed patterns should be tested whether the topological property (closeness) could facilitate symmetric detection.

Rosenholtz and colleagues proposed a texture tiling model in which they claimed that our visual system represents the periphery as a whole with textural compression (Balas, Nakano, & Rosenholtz, 2009; Rosenholtz et al., 2012). This indicates that our brain sacrifices irrelevant detail, while retaining sufficient information to facilitate much of what we commonly think of as vision and to direct later action. They adopted figures of Kimchi and Pirkner (2015) to generate mongrels with their high-dimension model (Rosenholtz, Yu, & Keshvari, 2019). When the central square formed of L junctions was flanked by the same shapes, the topological property between the target and flankers was the same. The crowding effect was worse than the topologically different condition where the L junctions formed a square being flanked by the L junctions that did not form a square. The model was consistent with the topological perception theory.

Our findings support the view that topological definition of objects provides a coherent account and is able to provide information for object identity in peripheral vision (Zhou et al., 2010). According to our results and topological perception theory, the substantial information we need for pattern recognition to form the perception of an object and direct our later action was specified by topological properties. With limited resolution in the periphery, our visual system extracts the topological properties sensitively that were perceived as an object.

Keywords: peripheral vision, pattern recognition, change detection, topological change

Acknowledgments

Supported in part by the National Nature Science Foundation of China grant (31730039), the Ministry of Science and Technology of China grant (2020AAA0105601, 2019YFA0707103), and the Chinese Academy of Sciences grants (XDB32010300, ZDBS-LY-SM028).

Commercial relationships: none.
Corresponding author: Bo Wang.
Email: bwang@ibp.ac.cn.
Address: Datun Rd. #15 Institute of Biophysics, CAS, Chaoyang District, Beijing, 100101, China.

References

Achtman, R. L., Hess, R. F., & Wang, Y. Z. (2000). Regional sensitivity for shape discrimination. *Spatial Vision, 13*, 377–391.

Azzopardi, P., Jones, K. E., & Cowey, A. (1999). Uneven mapping of magnocellular and parvocellular projections from the lateral geniculate nucleus to the striate cortex in the macaque monkey. *Vision Research, 39*(13), 2179–2189.

Balas, B., Nakano, L., & Rosenholtz, R. (2009). A summary-statistic representation in peripheral vision explains visual crowding. *Journal of Vision, 9*(12), 13, doi:10.1167/12.4.14.

Berardi, N., & Fiorentini, A. (1991). Visual field asymmetries in pattern discrimination: A sign of asymmetry in cortical visual field representation? *Vision Research, 31*(10), 1831–1836.

Boynton, R. M. (1979). *Human color vision*. New York, NY: Holt, Rinehart and Winston.

Brainard, D. H., & Vision, S. (1997). The psychophysics toolbox. *Spatial Vision, 10*, 433–436.

Carmody, D. P., Nodine, C. F., & Locher, P. J. (1977). Global detection of symmetry. *Perceptual and Motor Skills, 45*(3, Suppl.), 1267–1273.

Carrasco, M., Mcelree, B., Denisova, K., & Giordano, A. M. (2003). Speed of visual processing increases with eccentricity. *Nature Neuroscience, 6*(7), 699–670.

Castet, E., Keeble, D. R., & Verstraten, F. A. (2002). Nulling the motion aftereffect with dynamic random-dot stimuli: Limitations and implications. *Journal of Vision, 2*(4):3, 302–311.

Chen, C. M., Lakatos, P., Shah, A. S., Mehta, A. D., Givre, S. J., Javitt, D. C., . . . Schroeder, C. E. (2006) Functional anatomy and interaction of fast and slow visual pathways in macaque monkeys. *Cerebral Cortex, 17*, 1561–1569.

Chen, L. (1982). Topological structure in visual perception. *Science, 218*(4573), 699–700.

Chen, L. (2005). The topological approach to perceptual organization. *Visual Cognition, 12*(4), 553–637.

Connolly, M., & Essen, D. V. (1984). The representation of the visual field in parvicellular and magnocellular

layers of the lateral geniculate nucleus in the macaque monkey. *Journal of Comparative Neurology, 226*(4), 544–564.

Gheorghiu, E., Kingdom, F. A. A., Bell, J., & Gurnsey, R. (2011). Why do shape aftereffects increase with eccentricity?. *Journal of Vision, 11*(14), 18, doi:10.1167/11.14.18.

Harris, J. P., & Calvert, J. E. (1985). The tilt aftereffect: Changes with stimulus size and eccentricity. *Spatial Vision, 1*, 113–129.

Hartmann, E., Lachenmayr, B., & Brettel, H. (1979). The peripheral critical flicker frequency. *Vision Research, 19*(9), 1019–1023.

Hess, R. F., & Dakin, S. C. (1997). Absence of contour linking in peripheral vision. *Nature, 390*, 602–604.

Hess, R. F., & Dakin, S. C. (1999). Contour integration in the peripheral field. *Vision Research, 39*, 947–959.

Kimchi, R., & Pirkner, Y. (2015). Multiple level crowding: Crowding at the object parts level and at the object configural level. *Perception, 44*(11), 1275–1292.

Kveraga, K., Boshyan, J., & Bar, M. (2007). Magnocellular projections as the trigger of top-down facilitation in recognition. *Journal of Neuroscience, 27*(48), 13232–13240.

Lamme, V. A., & Roelfsema, P. R. (2000). The distinct modes of vision offered by feedforward and recurrent processing. *Trends in Neurosciences, 23*(11), 571–579.

Larson, A. M., & Loschky, L. C. (2009). The contributions of central versus peripheral vision to scene gist recognition. *Journal of Vision, 9*(10):6, 1–16, https://doi.org/10.1167/9.10.6.

Lennie, P. (1998). Single units and visual cortical organization. *Perception, 27*(8), 889.

Lettvin, J. Y. (1976). On seeing sidelong. *The Sciences, 16*, 10–20.

Levi, D. M. (2008). Crowding—An essential bottleneck for object recognition: A minireview. *Vision Research, 48*, 635–654.

Levi, D. M., & Klein, S. A. (1986). Sampling in spatial vision. *Nature, 320*, 360–362, https://doi.org/10.1038/320360a0.

Levi, D. M., & Klein, S. A. (1990). The role of separation and eccentricity in encoding position. *Vision Research, 30*, 557–585.

Makela, P., Whitaker, D., & Rovamo, J. (1993). Modelling of orientation discrimination across the visual field. *Vision Research, 33*, 723–730.

Maunsell, J. H., Nealey, T. A., & dePriest, D. D. (1990). Magnocellular and parvocellular contributions to responses in the middle temporal visual area (MT) of the macaque monkey. *Journal of Neuroscience, 10*, 3323–3334.

Melmoth, D. R., Kukkonen, H. T., Makela, P. K., & Rovamo, J. M. (2000). The effect of contrast and size scaling on face perception in foveal and extrafoveal vision. *Investigative Ophthalmology & Visual Science, 41*, 2811–2819.

Nugent, A. K., Keswani, R. N., Woods, R. L., & Peli, E. (2003). Contour integration in peripheral vision reduces gradually with eccentricity. *Vision Research, 43*, 2427–2437.

Pointer, J. S., & Hess, R. F. (1989). The contrast sensitivity gradient across the human visual field: With emphasis on the low spatial frequency range. *Vision Research, 29*(9), 1133–1151.

Rodieck, R. W. (1973). *The vertebrate retina: Principles of structure and function*. San Francisco, CA: Freeman.

Rosenholtz, R. (2014). Texture perception. *Oxford Handbook of Perceptual Organization, 167*, 186.

Rosenholtz, R. (2016). Capabilities and limitations of peripheral vision. *Annual Review of Vision Science, 2*(1), 437–457, https://doi.org/10.1146/annurev-vision-082114-035733.

Rosenholtz, R., Huang, J., Raj, A., Balas, B. J., & Ilie, L. (2012). A summary statistic representation in peripheral vision explains visual search. *Journal of Vision, 12*(4), 14, doi:10.1167/12.4.14.

Rosenholtz, R., Yu, D., & Keshvari, S. (2019). Challenges to pooling models of crowding: Implications for visual mechanisms. *Journal of Vision, 19*(7):15, 1–25, https://doi.org/10.1167/19.7.15.

Rovamo, J., & Virsu, V. (1979). An estimation and application of the human cortical magnification factor. *Experimental Brain Research, 37*, 495–510.

Saarinen, J. (1988). Detection of mirror symmetry in random dot patterns at different eccentricities. *Vision Research, 28*(6), 755–759.

Schmolesky, M. T., Wang, Y., Hanes, D. P., Thompson, K. G., Leutgeb, S., Schall, J. D., . . . Leventhal, A. G. (1998). Signal timing across the macaque visual system. *Journal of Neurophysiology, 79*(6), 3272–3278.

Strasburger, H., Harvey, L. O., & Rentschler, I. (1991). Contrast thresholds for identification of numeric characters in direct and eccentric view. *Perception and Psychophysics, 49*(6), 495–508.

Strasburger, H., Rentschler, I., & Harvey, L. O., Jr (1994). Cortical magnification theory fails to predict visual recognition. *European Journal of Neuroscience, 6*(10), 1583–1588.

Strasburger, H., Rentschler, I., & Jüttner, M. (2011). Peripheral vision and pattern recognition: A review. *Journal of Vision, 11*(5), 13, doi:10.1167/11.5.13.

Tangen, J. M., Murphy, S. C., & Thompson, M. B. (2011). Flashed face distortion effect: Grotesque faces from relative spaces. *Perception, 40*, 628–630.

Thomas, J. P. (1987). Effect of eccentricity on the relationship between detection and identification. *Journal of the Optical Society of America A, 4*, 1599–1605.

Virsu, V., Näsänen, R., & Osmoviita, K. (1987). Cortical magnification and peripheral vision. *Journal of the Optical Society of America A, 4*, 1568–1578.

Wagemans, J. (1997). Characteristics and models of human symmetry detection. *Trends in Cognitive Sciences, 1*(9), 346–352.

Wang, B., Zhou, T. G., Zhuo, Y., & Chen, L. (2007). Global topological dominance in the left hemisphere. *Proceedings of the National Academy of Sciences of the United States of America, 104*(52), 21014–21019.

Wertheim, T. (1894). About indirect vision. *Zeitschrift für Psychololologie und Physiologie der Sinnesorgane, 7*, 172–187.

Whitaker, D., Latham, K., Makela, P., & Rovamo, J. (1993). Detection and discrimination of curvature in foveal and peripheral vision. *Vision Research, 33*, 2215–2224.

Wichmann, F. A., & Henning, G. B. (1998). No role for motion blur in either motion detection or motion-based image segmentation. *Journal of the Optical Society of America A, 15*(2), 297–306.

Xi, H., Wu, R., Wang, B., & Chen, L. (2020). Topological difference between target and flankers alleviates crowding effect. *Journal of Vision, 20*(9):9, 1–12, https://doi.org/10.1167/jov.20.9.9.

Xing, J., & Heeger, D. J. (2000). Center-surround interactions in foveal and peripheral vision. *Vision Research, 40*, 3065–3072.

Zeeman, E. C. (1962). The topology of the brain and visual perception. In M. K. Fort (Ed.), *The topology of 3-manifolds* (pp. 240–256). Englewood Cliffs, NJ: Prentice-Hall.

Zhou, K., Luo, H., Zhou, T., Zhuo, Y., & Chen, Lin. (2010). Topological change disturbs object continuity in attentive tracking. *Proceedings of the National Academy of Sciences of the United States of America, 107*(50), 21920–21924.

Zhuo, Y., Zhou, T. G., Rao, H. Y., Wang, J. J., Meng, M., & Chen, M., ...Chen, L. (2003). Contributions of the visual ventral pathway to long-range apparent motion. *Science, 299*(5605), 417–420.